Amorphous nature of small CdS nanoparticles: Molecular dynamics simulations

Chad E. Junkermeier*,† and James P. Lewis
Department of Physics, West Virginia University, Morgantown, West Virginia 26506, USA

Garnett W. Bryant
National Institute of Standards and Technology, 100 Bureau Drive, Stop 8423, Gaithersburg, Maryland 20899-8423, USA

(Received 23 October 2008; revised manuscript received 5 January 2009; published 25 March 2009)

The semiconductor CdS is generally found in the wurtzite structure. Prior experimental and theoretical results confirm that the semiconductor CdS nanoparticles maintain a wurtzite structure for diameters greater than 6 nm. There is disagreement in the literature for sizes smaller than 6 nm. We use the density-functional theory FIREBALL code and perform finite-temperature molecular dynamics simulations on nanoparticles that are approximately 2 nm in diameter, considering different sized structures and different simulation temperatures. To determine the structure of the nanoparticles we analyze the radial distribution of the atoms about the center of the nanoparticle, the nearest-neighbor and next-nearest-neighbor bond lengths, and the radial distribution function about individual atoms. Comparing the molecular dynamics simulations of relaxed nanocrystals against bulklike wurtzite and zinc-blende nanocrystals, we find that small uncapped CdS nanoparticles are not nanocrystals but are amorphous.

DOI: 10.1103/PhysRevB.79.125323 PACS number(s): 73.22.−f, 61.46.Bc, 61.46.Hk, 71.15.Pd

I. INTRODUCTION

Semiconducting nanoparticles have optical and electronic properties that are unlike either bulk materials or molecules. These properties open up exciting new fields of research and development. It is expected that semiconductor nanoparticles can be used in novel applications for energy and lighting, disease detection, and solid-state quantum computing. Nanocrystals composed of type II-VI semiconductors are especially exciting because of their relatively large band gap. The novel properties of nanoparticles become more pronounced as the size becomes smaller than the exciton Bohr radius. For CdS nanoparticles this happens at a diameter of about 5 nm.[1]

The structure of CdS nanoparticles is an important factor for engineering optoelectronic devices where CdS nanocrystals are integrated with electronic platforms. Bulk CdS is found in the wurtzite (W) crystal structure. In nanoparticle form it may be found in the W structure or in the zinc-blende (ZB) crystal structure, or even in the rocksalt structure under high pressure. Experimental results suggest that the crystal structure of CdS nanoparticles is size dependent. At sizes smaller than 6 nm, there has been considerable disagreement in the literature. In this paper, we address, theoretically, this disagreement by determining the lattice structure of isolated colloidal nanoparticles that are about 2 nm in diameter.

Experimental results determining the structure (W or ZB) of colloidal CdS nanoparticles of about 2 nm in diameter are ambiguous. Using x-ray diffraction (XRD), high-resolution electron microscopy (HREM), and transmission electron microscopy (TEM), several groups have determined that nanoparticles near this size range are in a ZB structure.[2–4] Using XRD and solid-state nuclear magnetic resonance (NMR) Herron *et al.*[3] determined that particles less than 1.5 nm in diameter are amorphous with the nanoparticles becoming ZB by 2.5 nm in diameter and remain in a ZB structure through 3.5 nm. Murray *et al.*[5] used TEM, XRD, and selected area electron diffraction to determine that all of the nanoparticles they studied (CdS, CdSe, and CdSe) had a "predominantly" W structure. Bautista-Hernández *et al.*[6] used TEM and transmission electron diffraction (TED) to study particles that were from 0.5 to 8 nm in diameter. They state that in most cases the comparison of their experimental and theoretical values for exciton energy fits when the W structure is used in the theoretical calculation, but that a discrepancy in one of their samples might be because some of the smaller nanoparticles were in a ZB structure. Nanda *et al.*[1] created two thin-film samples of CdS nanoparticles on a quartz plates. Using XRD, Nanda *et al.*[1] found that they could not conclusively determine the structure of CdS nanoparticles that had diameters of 2.5 nm. One reason for these conflicting results is that for small clusters, especially for II-VI clusters, very few of their properties can be measured directly.[7] Bautista-Hernández *et al.*[6] suggested that the differences seen could be due to some condition(s) that biases the growth of the nanoparticles in W or ZB phase.

Further complicating the understanding is that little is said about the ligands that are capping the surfaces of the colloidal nanoparticles in experimental studies. Little information is available about the surface density of the ligands, which determines how big a role the ligands play in the crystal structure of the nanoparticles.

A number of groups have tried to theoretically determine the lattice structure of II-VI nanoparticles by looking at the ground-state configuration of the nanoparticles through a relaxation process. In each case, their nanoparticles were isolated. Based on their total energy per atom results, Joswig *et al.*[8–10] showed that there is a fluctuation as to which crystal structure is more stable as the nanocrystal size increases. Additionally, according to their results, there is very little difference in the total energy per atom between the W and ZB structures. Similar results were found for CdSe, InP, and ZnS.[11–13] Wen and Melnik[14] recently used *ab initio* methods to show that the ground state of relaxed CdS nanoparticles that start in a rocksalt structure has a lower energy, over a range of temperatures, than either a W or graphitic phase for nanoparticles that are about 1.3 nm along their longest di-

mension. Overall, these results show that the more stable crystal structure is highly size dependent. Starting in a W phase, adding a few atoms can change the phase from W to ZB and with the addition of a few more atoms back to W. There is also a material dependence, the change between W and ZB happens at different sizes for each material.

Finding the (zero-temperature) ground-state configuration of these nanoparticles is a first step in understanding the structure of the nanoparticles; however, using these results to claim that nanoparticles of a particular size are formed in a particular crystal structure is not sufficient. Two potential problems exist. First, the types of calculations performed do not necessarily find the global ground state. Rather, they find a local minimum. Finding local minima is problematic because the energy difference between the ZB and W structures is small and it is easy to imagine cases where the local minima found give the wrong indication as to the more stable configuration. Second, sources of enthalpy (temperature, free energy, etc.) play an important role in determining the stability of a crystal structure, but are not well represented in zero-temperature energy calculations.[2] Thus, while the results discussed in the preceding paragraph may be useful within their sphere of validity, they are insufficient for determining the structure of nanoparticles. This work focuses on simulations of small isolated CdS nanoparticles using long period finite-temperature molecular dynamics (MD) calculations. This type of MD simulation does not rely on finding a minimum energy in determining crystal structure, while it does include sources of enthalpy that are important factors in the stability of the structure.

Vorokh and Rempel[15] suggested that nanoparticles are noncrystalline. They calculated XRD patterns using a variety of crystal and noncrystalline close-packed structures (including W and ZB). Their structures consisted of layered hexagonal sheets of atoms, such that each sheet was displaced by some amount from its neighboring sheets. According to their results a noncrystalline close-packed structure, with a characteristic size of approximately 5 nm, most resembles the experimental XRD data. Our finite-temperature simulations for small nanoparticles support this finding.

In this paper we will discuss our results of finite-temperature MD simulations of isolated CdS nanoparticles, in the 2 nm diameter range. In Sec. II, we will discuss the theoretical basis of the MD simulations as well as describe some of the analysis techniques that we used. In Sec. III we will discuss the results of our simulations and how they can be interpreted. A summary and concluding remarks will be given in Sec. IV.

II. COMPUTIONAL METHODS

Primarily, we performed finite-temperature MD simulations at a desired set of temperatures to determine the effect of finite temperature on the expected atomic positions and bond lengths. A quick overview of the calculations performed is given here along with a flow chart (Fig. 1) to illustrate the order of the calculations, while a detailed description of the calculations is given in the subsequent paragraphs. Starting off with nanoparticles in bulklike W and ZB

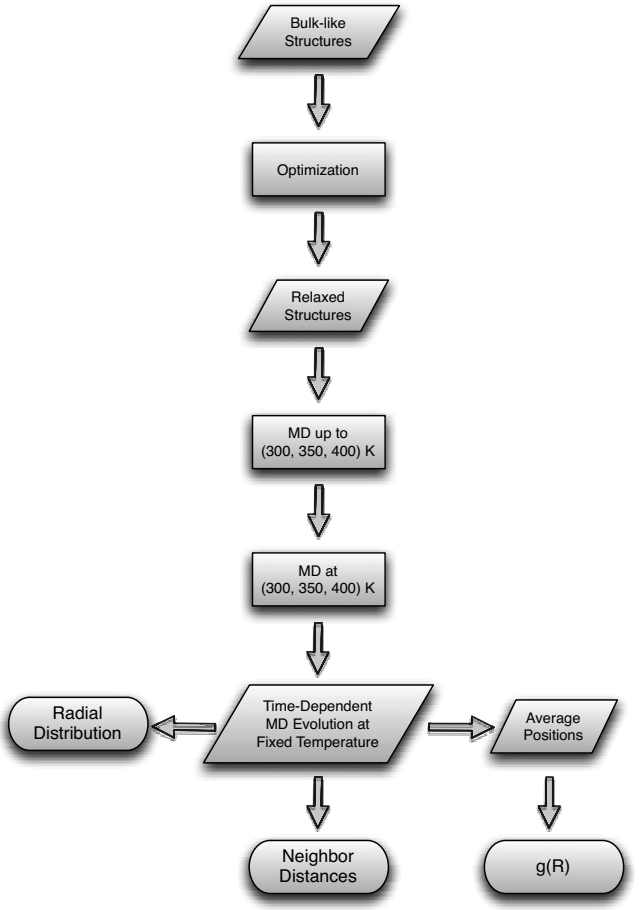

FIG. 1. A flow chart specifying the MD simulations and analysis performed. Atomic structures are shown as parallelograms, MD simulations are rectangles, and analysis results are given as ellipses.

structures, we optimize the nanoparticles' zero-temperature structure (allowing the bond lengths and bond angles to change, or even bond breaking or bond formation, so that the internal forces of the nanoparticles are minimized) by the use of a quenching procedure. We then performed two sequential MD simulations on the optimized (relaxed) structures: the first is to slowly increase their temperatures to some desired value and the second is fixed at the desired temperature. The fixed temperature evolutions are used to calculate characteristic properties of the nanoparticle systems.

We use the FIREBALL method, which is a density-functional theory (DFT) method based on local orbitals obtained from a pseudopotential to calculate the electronic structure and total energy.[16–18] FIREBALL can perform several different types of calculations, based on the method chosen and the approximations used, to compute the Hamiltonian matrix elements. For this work, we used the Harris-Foulkes functional[19,20] with the Horsfield exchange-correlation approximation.[21] The Harris-Foulkes functional is similar to the Kohn-Sham functional except that it gives a better approximation to the ground-state energy when the density ρ is not derived self-consistently. The input density is a sum of confined spherical atomiclike densities $\rho_{\text{in}}(\mathbf{r})=\Sigma_i n_i|\phi_i(\mathbf{r}-\mathbf{R}_i)|^2$, where the orbitals $\phi_i(\mathbf{r}-\mathbf{R}_i)$ are the basis functions used in solving the one-electron Schrödinger equation and n_i

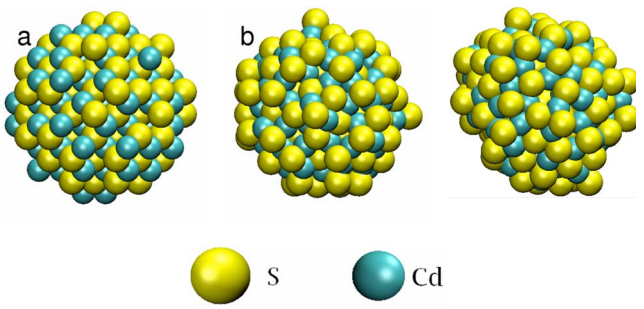

FIG. 2. (Color online) Structure of the nanoparticle of radius 1.164 nm, $Cd_{132}S_{132}$ when in the (a) zinc-blende structure (ZB264), (b) relaxed structure (RZB264), and (c) a representative time step (time step 6999) from the MD evolution at 300 K (CdS264). Each representation is viewed from the same angle and from the same distance.

have integer values equal to the number of electrons, in the respective shells, of the neutral atom.[22] In solving the one-electron Schrödinger equation we use a minimal basis set of local orbitals (a $4d^{10}5s^2$ basis for Cd and a $3s^23p^4$ basis for S). The wave function of each local orbital is defined to vanish at a cutoff radius (similar to an "atom in a box"). Cutoff radii used for the sulfur atoms are $r_c^s=4.2a_o$ and $r_c^p=4.7a_o$, where a_o is the Bohr radius. For the cadmium atoms, the radii are $r_c^s=5.1a_o$, $r_c^p=5.0a_o$, and $r_c^d=4.5a_o$. In a previous work we showed that this level of approximation gives reasonable values for the band gap and lattice constant of bulk CdS as well as nanocrystalline structures and band gaps that are supported by the findings of other groups.[23]

For the starting configurations of the nanoparticles, we consider spherical crystalline structures in a zinc-blende configuration. The initial structures included a bond-centered nanoparticle of radius 1.164 nm, $Cd_{132}S_{132}$ (ZB264), shown in Fig. 2(a); an anion-centered nanoparticle of radius 1.164 nm, $Cd_{140}S_{141}$ (ZB281); and an anion-centered nanoparticle of radius 1.362 nm, $Cd_{180}S_{177}$ (ZB357).[23] We applied a 600 time step MD quenching procedure, at 0 K, in order to relax the structure. The structural relaxation also partially passivates the surface. By partial passivation we mean that the ions move, so that some of the dangling bonds are passivated by other ions in the CdS nanoparticle. This decreases the metallization of the surface. Capping ligands are not included. The passivation is provided only by the surface relaxation. The relaxed versions of ZB264, ZB281, and ZB357 are, respectively, designated by RZB264 [Fig. 2(b)], RZB281, and RZB357. The total energy per atom is less after relaxation than before, showing that the relaxed configurations are more energetically favorable than the bulklike configurations. The comparison in Fig. 2 shows the degree of surface relaxation and hints at the degree of internal relaxation.

In the second step of calculations, we performed MD simulations to incrementally increase the temperature of the relaxed ZB nanoparticles up to 300 K (room temperature). We also increased the temperature of RZB281 to 350 and 400 K in separate calculations to simulate the effects of the elevated temperatures during growth. We have not yet considered higher temperatures because of the computational cost. The incremental increase in the temperature of the system with each time step, slowly changing the temperature from one time step to the next (in the range of 0.025–0.045 K per step). After each nanoparticle was raised to the desired temperature, each system underwent another MD simulation fixed at the desired temperature. We performed each simulation using a Nosé-Hoover thermostat, with each simulation covering 10 ps with a 1 fs time step. The output of each fixed temperature MD simulation is a MD evolution. When discussing the time-dependent MD evolution of a nanoparticle we will designate it by CdS264 [a representative atomic configuration is given in Fig. 2(c)], CdS281, or CdS357. When discussing CdS281 we will also specify the temperature of the system concerned.

When performing the MD calculations we used a number-volume-temperature (*NVT*) ensemble with an explicit velocity Verlet integrator in which a factorization of the Liouville operator is used to propagate the ionic positions. A Nosé-Hoover chain thermostat was used to control temperature.[24–27] The Hamiltonian is replaced with a non-conservative system that adds a series of damped oscillator terms to the potential energy. This conservative system cools (or heats) the system if the instantaneous kinetic energy is higher (or lower) than k_BT, where T is the desired temperature. This integrator is reversible in time, allows long time steps, and creates ergodic motion for evaluation of thermal averages. In the FIREBALL code the default settings have four thermostats in the Nosé-Hoover chain with a characteristic frequency of each damped oscillator that is set to 1.2 rad/fs.

We also looked at spherical wurtzite structures that were similar to the ZB structures: a bond-centered nanoparticle of radius 1.164 nm, $Cd_{124}S_{135}$ (W259); an anion-centered nanoparticle of radius 1.164 nm, $Cd_{138}S_{138}$ (W276); and an anion-centered nanoparticle of radius 1.362 nm, $Cd_{178}S_{159}$ (W337). We ran the same MD quenching procedure as was performed on the ZB nanoparticles to obtain relaxed structures. These relaxed structures where then subjected to the incremental increase in temperature and the fixed temperature MD simulations. For brevity we will not focus on these MD simulations in this paper, but the results were similar to what we discuss below.

To quantify how much the lattice structure of the CdS nanoparticles resembles the bulk W or the bulk ZB lattices, we must use statistical measures. One of these is the chi-squared statistic, which is a measure of the deviation of a sample from its expected value.[28,29] If n samples are taken from a normal population then

$$\chi^2 = \sum_i^n \frac{(R_i - \mu)^2}{\sigma}, \tag{1}$$

where R_i is the result of a sample, μ is the mean value, and σ is the standard deviation.

In particular, we use chi squared to compare two sets of binned data, R and S (this can be thought of as a measure of how closely related two histograms are), where the number of data elements in R is not equal to the number of data elements in S. The form of chi squared in this case is

$$\chi^2 = \sum_i^n \frac{(\sqrt{S/R}R_i - \sqrt{R/S}S_i)^2}{(R_i + S_i)}, \quad (2)$$

where we have n bins, $R=\Sigma_i^n R_i$, and $S=\Sigma_i^n S_i$. When we use the chi-squared statistic below, we will have formed binned data out of the radial distance of the atoms from the center of the nanoparticle. This binned data will be R_i and the binned data of either the W or ZB structure will be S_i in Eq. (2). The best fit happens when $\chi^2=0$, and as χ^2 grows larger the fit becomes worse. When we use this in our analysis below, χ^2 will be used to measure the similarity of each time step of the MD evolutions to the W or ZB structure.

The chi-squared statistic for binned data was derived under the assumption that all of the bins have nonzero values. We will be using it under conditions where for some set of bins $\{j|j\subset i\}$ the values of R_j and S_j are both zero, causing the denominator of Eq. (2) to be equal to zero. To get around this problem we will define each term of chi squared to be equal to zero at these points;

$$\chi_i^2 = \begin{cases} 0, & \text{if } R_i = 0 = S_i, \\ \dfrac{(\sqrt{S/R}R_i - \sqrt{R/S}S_i)^2}{(R_i + S_i)}, & \text{otherwise}, \end{cases} \quad (3)$$

where $\chi^2=\Sigma_i^n \chi_i^2$. Thus, whereas the traditional chi-squared statistic was defined to be used with a normal distribution that was assumed to be positive everywhere, we are allowing for distributions that also contain bins with values of zero.

The chi-squared statistic provides a means for determining if the data set can be related to the hypothesized sample. This determination is made by comparing the chi-squared value with some critical value. If the chi-squared value is less than the critical value then we accept the "null hypothesis;" in our case, that the MD simulation conforms to the reference system W or ZB. If the chi-squared value is greater than the critical value then we reject the null hypothesis and accept the "alternate hypothesis" that the MD simulation does not conform to the reference system.

To find the critical value, we first determine the number of bins used. Subtracting one from the number of bins used we obtain the degrees of freedom (a statistical term that is unrelated to the phase-space degrees of freedom). Once we have determined the degrees of freedom we can use look up tables from an introductory statistics book to obtain the critical value.[29] Table I contains the degrees of freedom and critical values that we will use later. We chose to use critical values that give us a 95% surety of correctly rejecting the null hypothesis.

TABLE I. Regions used to sample the nanoparticles. We give here the values needed when using the chi-squared statistic to determine quality of fit against binned data (Ref. 29). "DOF" indicates degrees of freedom and "CV" indicates the critical value. The critical values given in CV represent being able to reject the null hypothesis with a 95% degree of certainty.

Radius (nm)	Bins	DOF	CV
$r\leq 0.5$	10	9	16.92
$0.5<r\leq 0.9$	7	6	12.59
$0.9<r\leq 1.3$	8	7	14.07
$r\leq 1.3$	25	24	36.41

III. RESULTS

In analyzing the results, we examine four regions of the nanoparticle, based on radial distance from the center of the nanoparticle. These regions are $r\leq 0.5$ nm, $0.5<r\leq 0.9$ nm, $0.9<r\leq 1.3$ nm (the region initially including the surface), and $r\leq 1.3$ nm. Our choice is based on the expectation that the atoms at the center of the nanoparticle would behave differently than the atoms on the surface. The region nearest the origin is slightly larger in radius than the next two regions, so that the central region has enough atoms for the results to have statistical meaning. We use these regions throughout this paper.

The first type of analysis we consider is the radial distribution of the nanoparticle's atoms from the center of the nanoparticle. This is different from the radial distribution function $g(R)$, which will be discussed later. The distribution data were condensed into histogram binned data for easier data analysis. In Fig. 3(a) we show the binned data of the bulklike W and ZB structures, where we used 100 bins over $0<r\leq 1.3$ nm.

In Fig. 3(b) we compare the radial distribution of the atoms in the bulklike ZB structure with the radial distribution of the same atoms during a sample time step from a MD simulation. We find that even though an atom starts in a particular region, it does not necessarily stay in that region. Since the atoms may not stay in the region where they started, we must allow for the possibility that atoms exchanged positions, leaving the structure of the nanoparticle unchanged, as we analyze the MD simulations. To do this we determined which atoms are in each region during each time step of a MD simulation.

We turn now to analyzing the MD simulations. We computed the radial distribution of the atoms in the nanoparticles for each time step in the MD evolutions. Here we used 25 bins over $0<r\leq 1.3$ nm. The 25 bins that we use here have more atoms per bin, which is desirable for the chi-squared statistic that we use, whereas the 100 bins that we use for Fig. 3 show where atoms are located. The binned data of each time step were then compared with the binned data of both the W and ZB structures using the chi-squared statistic. In Fig. 4 we show a representative data set (CdS281 at 300 K); the critical value (given in Table I) is given by the dashed line.

On the left side of Fig. 4 we have a plot of chi squared as a function of time. The box plots on the right side summarize the data on the left. The thick center line of the box plot gives the median value, the top and bottom edges of the box give the quartiles, and the whiskers show the rest of the data. Each row of Fig. 4 gives the chi-squared data for a different region of the nanoparticle. In Fig. 5, we show the summarized data for each of the systems that we have studied.

Figure 5 shows that the average chi squared is above the critical value in all cases. As stated earlier, if the chi-squared value is greater than the critical value then the MD simula-

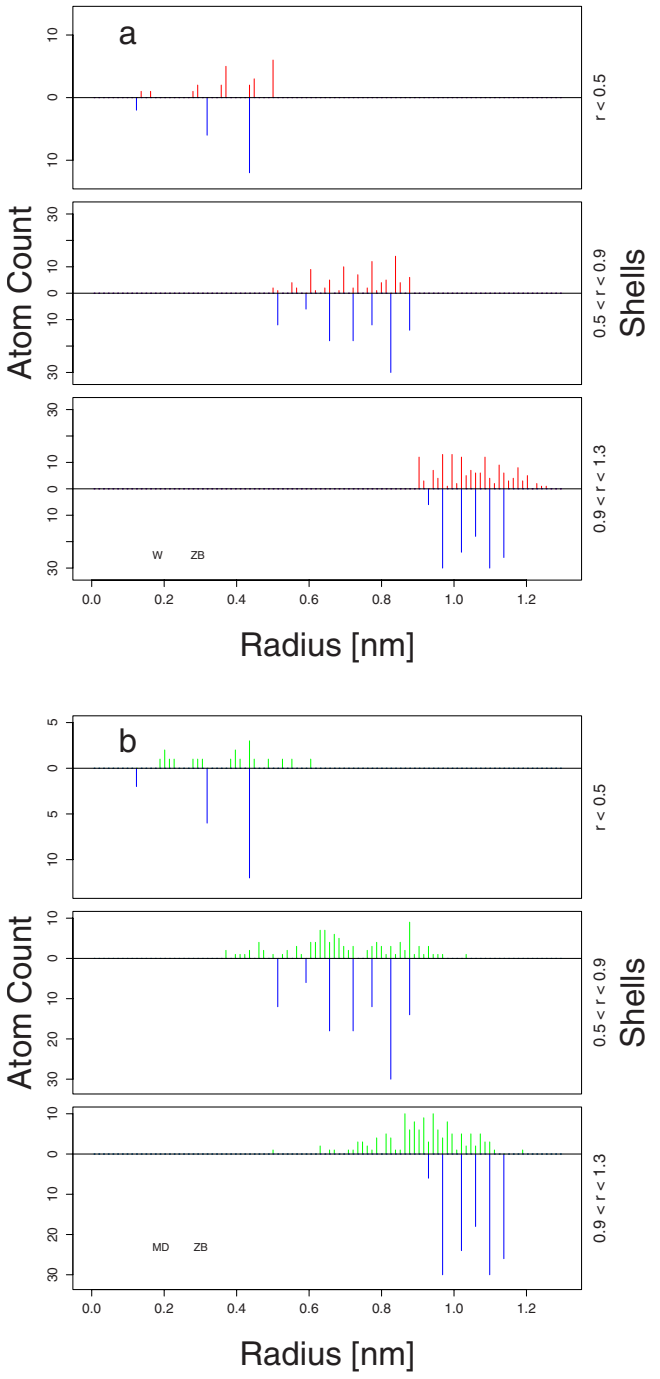

FIG. 3. (Color online) Radial distribution of atoms. (a) The radial distribution of the bond-centered W259 and ZB264 bulklike structures. (b) This is a representative time step from CdS264, which shows how the atoms that were originally in the ZB264 positions are spread out during a MD simulation.

tion does not conform to the reference system. Therefore, according to the radial distribution, the MD simulations do not correspond to either the W or ZB structure.

We computed the nearest-neighbor distances by finding the distance between an atom and all of the other atoms in the nanoparticle for each time step. An atom was determined to be a nearest neighbor if it was of the other species and if it was closer than 0.27 nm from the first atom (for a maximum distance that is about 20% longer than the bulk nearest-neighbor distance of either W or ZB).

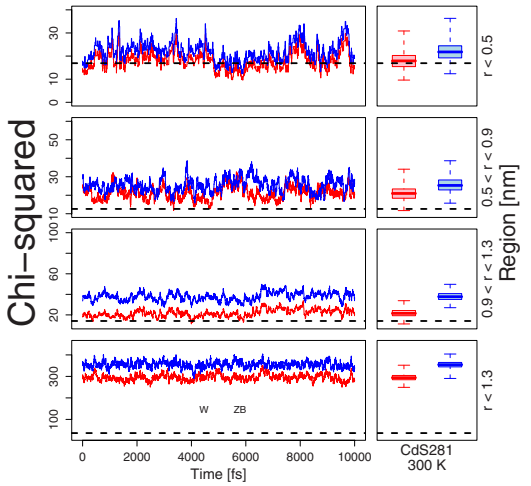

FIG. 4. (Color online) Plots comparing the chi-squared fit of the MD results against W and ZB. The rows are for the MD simulations. The columns specify the region of the nanoparticles that is being compared.

Figure 6(a) presents a box plot representation of the nearest-neighbor distances measured over the course of each MD simulation (the size of each sample set used to produce the box plot, for each region, is 10^5–10^6 data points). Again, the thick center line of the box plot gives the median value, the left and right edges of the box give the quartiles, and the whiskers show the rest of the data. The results are given by region. We find that the median nearest-neighbor distance near the nanoparticle surface is close to the W nearest-neighbor distance, while the interior regions do not resemble either W or ZB. Because it is possible to directly measure the nearest-neighbor distance of the surface atoms of nanoparticles, this may be the reason why others have found that CdS nanoparticles of this size are in a W structure.

Figures 6(b) and 6(c) give the box plot representation of the Cd-Cd and S-S next-nearest-neighbor distances, respec-

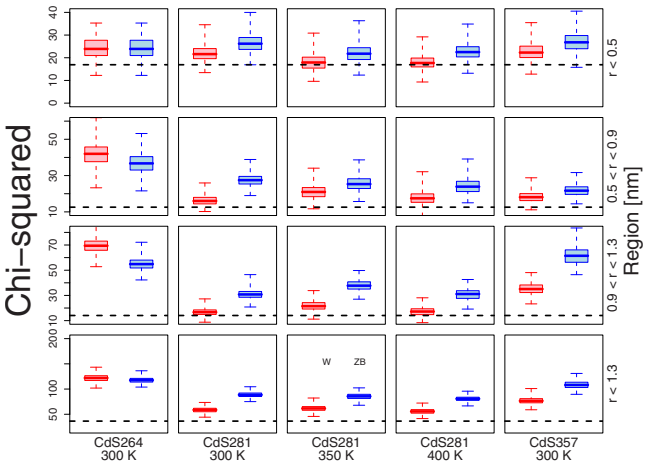

FIG. 5. (Color online) Bar plots comparing the chi-squared fit of the MD results against W and ZB. The rows are for the different regions of the nanoparticles that are being compared.

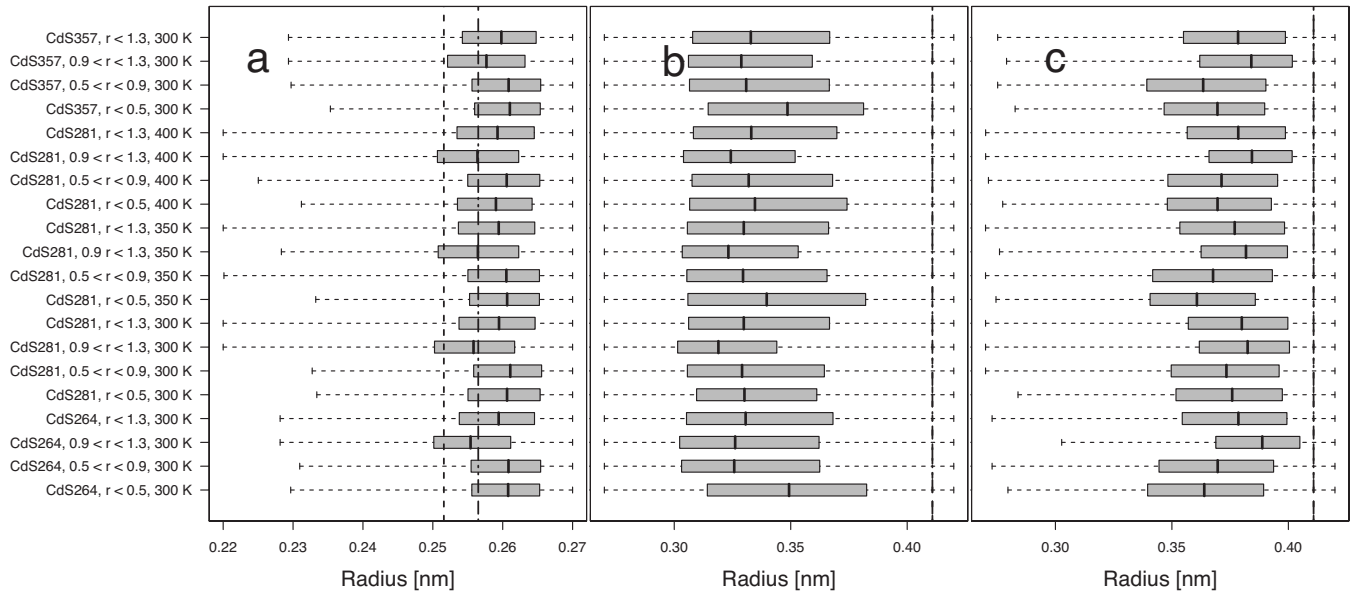

FIG. 6. (a) The nearest-neighbor distance and the next-nearest-neighbor distances for (b) Cd-Cd bonds and (c) S-S bond for each MD simulation. The vertical dashed line represents the respective bond distance in ZB while the line with a long dash followed by two short dashes represents the bond distance in W. The bold black line within the boxes gives the median value, left and right edges of the boxes show the quartiles while the whiskers represents the full range of values. In (b) and (c) W and ZB next-nearest-neighbor distances overlap.

tively. Our analysis shows that the next-nearest-neighbor distances in the MD evolutions are shorter than the corresponding nearest-neighbor distances for bulk W or ZB CdS. The average Cd-Cd distance is shorter by about 15%–21%, while the average S-S distance is shorter by about 5%–12%.

The results that we have presented here appear to correspond to the results shown in Fig. 3 of Wen and Melnik.[14] In their figure, they present a histogram of the bond lengths between 0.22 and 0.34 nm. In most of the cases that they present, there is a peak around the nearest-neighbor distance and another smaller peak around where we find the Cd-Cd next-nearest-neighbor distance.

Earlier we discussed the radial distribution of atoms with the origin at the center of a nanoparticle. We now consider the radial distribution function $g(R)$, which is the radial distribution of atoms around a particular atom. The radial distribution function is often used to determine if a system is crystalline or amorphous. Crystal structures have long-range order. If a system is crystalline then there would be several sharp peaks representing the distances to the nearest neighbors and the next-nearest neighbors with additional peaks for extended neighbors at higher radii. Amorphous structures have an absence of long-range order. When $g(R)$ of an amorphous structure is computed, there may be any number of broadened shell-like distributions, but there are no regions where there is an absence of neighbors.[30]

To compute $g(R)$, we first computed the average position of each atom of a system for each of the MD evolutions. $g(R)$ was then computed on each system (CdS264, CdS281, and CdS357) using the average position of the atoms from the respective evolution. If we had instead used the values obtained by plotting $g(R)$ of all the time steps in one graph, we would expect to see a broader distribution of atoms, due to the diffusion during the time evolution, than what we see for bulklike W and ZB structures. By using the average positions, if we find a diffuse $g(R)$ then this is because of the structure of the nanoparticle and is characteristic of an amorphous structure.

To show that this line of reasoning is justified, we optimized a supercell of bulk zinc-blende CdS, linearly increased the temperature of the system using a MD simulation, and then ran a 10 000 time step MD simulation at 300 K. We then computed the average position of the atoms in the supercell and computed the radial distribution function. The resultant graph of the radial distribution function had sharp peaks similar to what is found in the far right column of Fig. 7. Thus, this method of computing $g(R)$ gives the expected crystal structure result.

As shown in Fig. 7, we find that in the $r \leq 0.5$ nm region most of the distribution is close to the nearest-neighbor peak, with no gap between the nearest-neighbor and next-nearest-neighbor peaks. The $0.5 < r \leq 0.9$ nm region is similar to the $r \leq 0.5$ nm region in that there is no gap but there are also more neighbors further away from the reference atom. This is because there are more atoms in this region. The $0.9 < r \leq 1.3$ nm region has a broad distribution in the outer regions but also shows sharper next-nearest-neighbor peaks and gaps in the cases of CdS264 and CdS281 and 350 K. This may indicate that there is short-range order on the surface of the nanoparticles, which is consistent with what we discussed about the nearest-neighbor distance as found in Fig. 6. However, the sharper structure near the surface is also likely due to the fewer atoms in the distribution about an atom and thus less broadening. As we see, that for the overall nanoparticle $r \leq 1.3$ nm, the radial distribution function has a broad distribution with no gap, indicating that nanoparticle is in an amorphous structure.

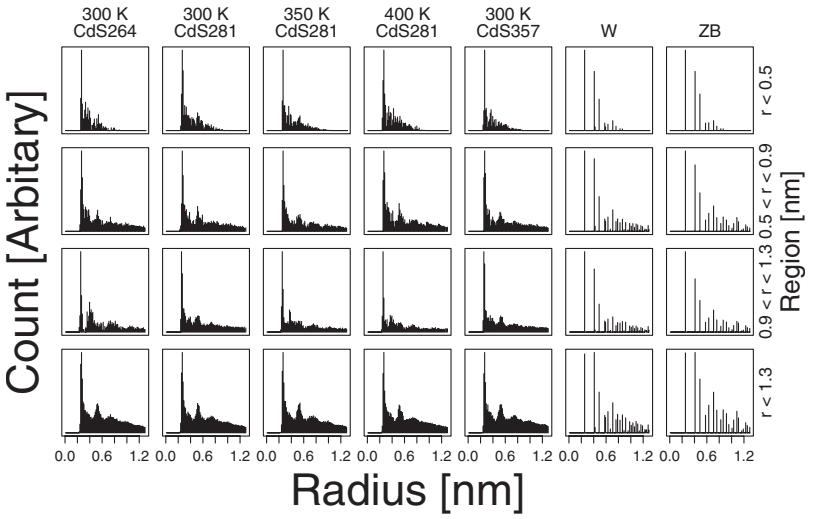

FIG. 7. Radial distribution function $g(R)$ for the nanoparticles. The last two columns on the right represent the $g(R)$ for W and ZB structures.

IV. SUMMARY

In summary, we used *ab initio* MD simulations to model small CdS nanoparticles of about 2 nm in diameter. Using the radial distribution of the atoms in the nanoparticles we employed a chi-squared statistic to show that the nanoparticles could not be in a W or ZB structure. The nearest-neighbor bond lengths do not resemble either W or ZB. Computing the radial distribution function $g(R)$, we found that the nanoparticle systems have an amorphous structure. Therefore, for the size that we considered, we find that isolated colloidal nanoparticles are *not* nanocrystals but are amorphous nanoparticles that appear to have short-range order on the surfaces. Our results agree with the findings of Vorokh and Rempel.[15] We expect that this amorphous nature will disappear for larger nanoparticles with diameters near 6 nm, where all of the experimental results we know agree that the nanoparticles are in the W structure. The amorphous structure may change or disappear when a capping layer passivates the nanoparticle.

ACKNOWLEDGMENTS

The MD simulations used in the relaxation of the nanoparticles in this work were performed at the Ira and Marylou Fulton Supercomputing Laboratory at Brigham Young University.

*chad.junkermeier@mail.wvu.edu
†Also at Department of Physics and Astronomy, Brigham Young University, Provo, UT 84602, USA.

[1] J. Nanda, B. A. Kuruvilla, and D. D. Sarma, Phys. Rev. B **59**, 7473 (1999).
[2] R. J. Bandaranayake, G. W. Wen, J. Y. Lin, H. X. Jiang, and C. M. Sorensen, Appl. Phys. Lett. **67**, 831 (1995).
[3] N. Herron, Ying Wang, and Hellmut Eckert, J. Am. Chem. Soc. **112**, 1322 (1990).
[4] R. Banerjee, R. Jayakrishnan, and P. Ayyub, J. Phys.: Condens. Matter **12**, 10647 (2000).
[5] C. B. Murray, D. J. Norris, and M. G. Bawendi, J. Am. Chem. Soc. **115**, 8706 (1993).
[6] A. Bautista-Hernández, G. Loaiza-González, L. Meza-Montes, and U. Pal, Sol. Energy Mater. Sol. Cells **79**, 539 (2003).
[7] M. C. Troparevsky, L. Kronik, and J. R. Chelikowsky, Phys. Rev. B **65**, 033311 (2001).
[8] J. Joswig, M. Springborg, and G. Seifert, J. Phys. Chem. **104**, 2617 (2000).
[9] J. Joswig, G. Seifert, T. A. Niehaus, and M. Springborg, J. Phys. Chem. B **107**, 2897 (2003).
[10] J. Frenzel, J. Joswig, and G. Seifert, J. Phys. Chem. C **111**, 10761 (2007).
[11] P. Sarkar and M. Springborg, Phys. Rev. B **68**, 235409 (2003).
[12] S. Roy and M. Springborg, J. Phys. Chem. **107**, 2771 (2003).
[13] S. Pal, B. Goswami, and P. Sarkar, J. Chem. Phys. **123**, 044311 (2005).
[14] B. Wen and R. V. N. Melnik, Appl. Phys. Lett. **92**, 261911 (2008).
[15] A. S. Vorokh and A. A. Rempel, Phys. Solid State **49**, 148 (2007).
[16] J. P. Lewis, K. R. Glaesemann, G. A. Voth, J. Fritsch, A. A. Demkov, J. Ortega, and O. F. Sankey, Phys. Rev. B **64**, 195103 (2001).
[17] P. Jelinek, H. Wang, J. P. Lewis, O. F. Sankey, and J. Ortega, Phys. Rev. B **71**, 235101 (2005).
[18] J. B. Keith, J. R. Fennick, C. E. Junkermeier, D. R. Nelson, and J. P. Lewis, Comput. Phys. Commun. **180**, 418 (2009).
[19] J. Harris, Phys. Rev. B **31**, 1770 (1985).
[20] W. M. Foulkes and R. Haydock, Phys. Rev. B **39**, 12520 (1989).
[21] A. P. Horsfield, Phys. Rev. B **56**, 6594 (1997).
[22] A. A. Demkov, J. Ortega, O. F. Sankey, and M. P. Grumbach, Phys. Rev. B **52**, 1618 (1995).
[23] C. E. Junkermeier, J. P. Lewis, and G. W. Bryant, Phys. Rev. B **77**, 205125 (2008).
[24] S. Nosé, J. Chem. Phys. **81**, 511 (1984).

[25] W. G. Hoover, Phys. Rev. A **31**, 1695 (1985).
[26] G. J. Martyna, M. E. Tuckerman, D. J. Tobias, and M. L. Klein, Mol. Phys. **87**, 1117 (1996).
[27] The CPMD Consortium, *Car-Parrinello Molecular Dynamics: An Ab Initio Electronic Structure and Molecular Dynamics Program* (MPI für Festkörperforschung and IBM Research Laboratory, Zürich, 2008).
[28] J. C. Davis, *Statistics and Data Analysis in Geology* (Wiley, New York, 1986).
[29] A. F. Siegel, *Statistics and Data Analysis: An Introduction* (Wiley, New York, 1988).
[30] S. R. Elliott, *Physics of amorphous materials* (Longman, New York, 1990).